circKMT2D contributes to H_2O_2-attenuated osteosarcoma progression via the miR-210/autophagy pathway

JUN ZHANG, XUBIN CHOU, MING ZHUANG, CHENLEI ZHU, YONG HU, DONG CHENG and ZHIWEI LIU

Department of Spine Surgery, The Third Affiliated Hospital of Soochow University, Changzhou 213001, P.R. China

Received August 4, 2019; Accepted June 10, 2020

DOI: 10.3892/etm.2020.9193

Abstract. Circular RNAs (circRNAs) have been demonstrated to be involved in osteosarcoma (OS) development; however, the underlying mechanism of circKMT2D in OS progression remains unclear. The present study aimed to elucidate how circKMT2D could affect hydrogen peroxide (H_2O_2)-induced OS progression. H_2O_2 (100 μmol/l) was used to treat MG63 and U2OS cells. The cell viability, invasive ability, apoptosis and circKMT2D expression were detected using Cell Counting Kit-8 assay, Transwell assay, flow cytometry and reverse transcription-quantitative PCR, respectively. Furthermore, MG63 and U2OS cells transfected with circKMT2D short hairpin RNA and negative control were treated with H_2O_2, and circKMT2D expression and cell phenotype were determined. Dual-luciferase reporter assay was conducted to determine the association between circKMT2D and miR-210 expression level. Rescue experiments were conducted to examine the mechanisms through which circKMT2D and miR-210 could affect H_2O_2-treated MG63 cells. In addition, the effects of miR-210 on the expression of the autophagy-related proteins Beclin1 and p62 in H_2O_2-treated MG63 cells were detected by western blotting. An autophagy inhibitor was used to treat the MG63 cells, and whether miR-210 could affect the H_2O_2-treated MG63 cell phenotype through autophagy was investigated. The results demonstrated that H_2O_2 treatment promoted cell apoptosis and decreased cell viability, invasive ability and circKMT2D expression in MG63 and U2OS cells. Furthermore, circKMT2D knockdown decreased the cell viability and invasive ability and enhanced the apoptosis of H_2O_2-treated MG63 and U2OS cells. circKMT2D possessed binding sites for miR-210 and inhibited miR-210 expression. In H_2O_2-treated MG63 cells, miR-210 silencing partially reversed the circKMT2D knockdown-induced cell viability inhibition and apoptosis promotion. In addition, miR-210 elevated Beclin1 expression and decreased p62 expression in H_2O_2-treated MG63 cells. The use of the autophagy inhibitor partially reversed the miR-210 overexpression-induced promotion of apoptosis and inhibition of the viability and invasive ability of H_2O_2-treated MG63 cells. Taken together, these findings indicated that circKMT2D knockdown may contribute to the inhibition of H_2O_2-attenuated OS progression via miR-210/autophagy pathway.

Correspondence to: Dr Zhiwei Liu, Department of Spine Surgery, The Third Affiliated Hospital of Soochow University, 185 Juqian Street, Changzhou 213001, P.R. China
E-mail: zhiweiliu1213@163.com

Key words: osteosarcoma, circKMT2D, miR-210, autophagy, tumorigenesis

Introduction

Osteosarcoma (OS) is a type of malignant tumor that often occurs in children and adolescents (1). As previously reported, the prevalence rate of OS increases by 0.3% per year (2). Similar to several other human malignancies, a high mortality rate, recurrence and metastasis are key factors leading to the poor prognosis of patients with OS (3). Surgical resection combined with adjuvant therapy, including chemotherapy and radiotherapy, has been reported to improve the prognosis of patients with OS to a certain degree (4). However, over the past two decades, no evident improvements have been observed in the survival rates of these patients (5).

Oxidative stress refers to an increased cell production of free radicals, including reactive oxygen species, ultimately resulting in damage to cells and tissues (6). A previous study demonstrated that tumor cells can be destroyed by increased oxidative stress (7). Inducing tumor cell apoptosis via increased oxidative stress may therefore be consider as a promising therapeutic strategy for malignancies (7). Hydrogen peroxide (H_2O_2) is a main intermediate of oxidative stress and is considered as a potent oxidant that induces cell senescence (8). In OS, it has been reported that treatment with 100 μM H_2O_2 decreases the viability and enhances the apoptosis of MG63 cells (9). However, the underlying mechanisms of H_2O_2 interference with OS cell phenotype remains unclear.

Circular RNA (circRNA) is a type of non-coding RNA that was discovered decades ago (10,11). Increasing evidence indicates that circRNAs play an important role in the development of human tumors (12). Salmena *et al* (13) proposed the competitive endogenous RNA mechanism (ceRNA mechanism) theory that gene transcripts, such as long-chain non-coding RNA, can influence mRNA expression by binding microRNAs (miRs) through competitive sponge attachment. In recent years, circRNAs have also been found to regulate mRNA expression through miRNA adsorption (14). A previous study has

demonstrated that circ_0002052 inhibits OS progression by sponging miR-1205 (15). Huang *et al* (16) reported that circ-NASP upregulates Forkhead box F1 expression by sponging miR-1253 in OS cells, thereby regulating the development of OS. These findings suggest that circRNAs could play a crucial role in the development of OS.

circKMT2D (also known as circRNA9920) is a recently discovered circRNA (17); however, its role in human tumors, including OS, remains unknown. In particular, we previously determined that circKMT2D expression is abnormally upregulated in H_2O_2-treated OS cells *in vitro* and that circKMT2D knockdown in H_2O_2-treated OS cells markedly decreased OS cell viability. Subsequently, it was hypothesized that circKMT2D could serve a regulatory role in the progression of OS. The effect of circKMT2D on H_2O_2-treated OS cell phenotype was therefore investigated in the present study. Furthermore, the role of miRNAs in regulating key pathways related to tumorigenesis may provide a powerful novel tool for diagnosis and targeted therapy. miR-210 has been reported to be involved in the occurrence and development of various types of cancer, including bladder cancer, glioblastoma and hepatocellular carcinoma (18-20). The clinical treatment of human tumors is in urgent need for the development of novel strategies to provide novel and reliable biomarkers and therapeutic targets (21). Therefore, the mechanisms through which circKMT2D may affect H_2O_2-attenuated OS cell progression were investigated by exploring the miR-210/autophagy pathway in the present study.

To the best of our knowledge, the present study was the first to investigate the role of circKMT2D in the progression of H_2O_2-attenuated OS cells. The findings from the present study may provide new insights into OS progression and may therefore provide a novel theoretical basis and a potential effective target for OS therapy.

Materials and methods

Cell lines. MG63 and U2OS cell lines were provided by The Cell Bank of Type Culture Collection of the Chinese Academy of Sciences. Cells were cultured in DMEM (Gibco; Thermo Fisher Scientific, Inc.) supplemented with 10% FBS (Gibco; Thermo Fisher Scientific, Inc.), 100 U/ml penicillin (Thermo Fisher Scientific, Inc.) and 100 μg/ml streptomycin (Thermo Fisher Scientific, Inc.) and placed at 37˚C in a humidified incubator containing 5% CO_2.

Cell treatment with H_2O_2. MG63 and U2OS cells in the logarithmic phase were collected and prepared as dispersed cell suspensions in DMEM complete medium containing 100 μmol/l H_2O_2 (Beijing Solarbio Science & Technology Co., Ltd.) for 24 h at 37˚C (22). The density of each cell suspension was $2x10^6$ cells/ml and each cell suspension was seeded into 6-well plates at a volume of 1 ml. All plates were maintained in an incubator at 37˚C and 5% CO_2.

Transfection. MG63 and U2OS cells in the logarithmic phase were collected and seeded in 6-well plates at a density of $5x10^5$ cells/well. A total of 1 ml serum-free DMEM medium was then added into each well. When the cell confluence rate reached ~70%, MG63 and U2OS cells were transfected with 10 nM circKMT2D short hairpin (sh)RNA (shcircKMT2D group; 5'-UGAUGAAUGCCGGCUCUAG-3') and negative control (shNC group; 5'-UGACGGAUGCACGCUCUAG-3') using Lipofectamine™ 2000 transfection reagent (Thermo Fisher Scientific, Inc.). In addition, MG63 cells were subjected to transfection with 10 nM miR-210 mimic (miR-210 mimic group; 5'-UCAGUCCAUGGUAGAACUUCG-3'), miR-210 inhibitor (miR-210 inhibitor group; 5'-UCGCUUGUGUCAGGUCCGCAA-3') and miR-210 NC (NC group; 5'-GGACCGUAGCCACUGUGAGUU-3'), respectively. Furthermore, pcDNA3.1-circKMT2D vector (10 nM) was used to transfect the MG63 cells (pcDNA3.1-circKMT2D group). Co-transfection was also performed on the MG63 cells using 10 nM circKMT2D shRNA and 10 nM miR-210 inhibitor simultaneously (shcircKMT2D + miR-210 inhibitor group). All plates were maintained in an incubator at 37˚C and 5% CO_2 for 6 h of transfection. Transfection was conducted using Lipofectamine® 2000 (Invitrogen; Thermo Fisher Scientific, Inc.) according to the manufacturer's protocol. The transfection efficiency was measured by reverse transcription-quantitative (RT-q)PCR. Subsequently, transfected cells were cultured in DMEM containing 10% FBS at a volume of 1 ml and were placed at 37˚C and 5% CO_2 for 48 h. circKMT2D shRNA, shRNA NC and pcDNA3.1-circKMT2D vector were purchased from Genechem, Inc. miR-210 mimic, miR-210 inhibitor and miR-210 NC were provided by Shangai GenePharma Co., Ltd..

Autophagy inhibitor treatment. MG63 cells in the miR-210 mimic group were incubated with DMEM complete medium containing 12.5 μg/ml 3-methyladenine (3-MA; Sigma-Aldrich; Merck KGaA) for 12 h at 37˚C and 5% CO_2. These cells constituted the miR-210 mimic + 3-MA group.

Cell counting kit-8 (CCK-8) assay. Cells cultured at 48 h post-transfection were harvested and seeded in 96-well plates at a density of $2x10^3$ cells/well. Cells were incubated with 100 μl DMEM complete medium containing or not 100 μmol/l H_2O_2 for 48 h at 37˚C. Subsequently, 10 μl CCK-8 solution (Dojindo Molecular Technologies, Inc.) was added to each well at 37˚C for 2 h before reading the absorbance at 450 nm using a microplate reader. Each sample was assessed in triplicate and the experiments were repeated three times.

Transwell assay. Transwell assay was performed using an 8-μm polycarbonate filter culture chamber (96-well plates; EMD Millipore) pre-plated with Matrigel for 1 h at room temperature. At 48 h post-transfection, cells were harvested and were seeded in the upper chamber of the chamber at the density of $2x10^5$ cells per well. Serum-free DMEM (100 μl, with or without 100 μM H_2O_2) was also added to the upper chamber. The lower chamber was filled with 500 μl DMEM complete medium with three replicate wells per group. Cells were cultured for 36 h at 37˚C and 5% CO_2. After the non-invasive cells were removed, the invading cells were washed twice with PBS, fixed for 10 min with 4% paraformaldehyde at room temperature for 20 min and stained with 0.1% crystal violet for 5 min. The invading cells were placed under a light microscope (Nikon Corporation; magnification, x200) and photographed.

Apoptosis detection. Cells cultured for 48 h were washed with PBS, harvested and centrifuged at room temperature for 5 min at 1,000 x g. A total of 500 μl binding buffer was used to resuspend the cells, and 5 μl AnnexinV-fluorescein isothiocyanate (FITC; cat. no. 40302ES20; Shanghai Yeasen Biotechnology Co., Ltd.) and 10 μl propidium iodide (PI) were then added to the cells. Cells were evenly mixed with the reagent and were stored in the dark for 15 min at room temperature. The apoptosis rate of each cell sample was measured by flow cytometry (BD Biosciences) and analyzed using FlowJo software (version 7.6.1; FlowJo LLC).

RT-qPCR. Total RNA was extracted from the cells using TRIzol reagent (Invitrogen; Thermo Fisher Scientific, Inc.) and reverse transcribed into a cDNA template busing the reverse transcription kit (Applied Biosystems; Thermo Fisher Scientific, Inc.) according to the manufacturers' instructions. The PCR amplification reaction was carried out using cDNA as template with the following conditions: 95˚C for 10 min, 95˚C for 15 sec, 62˚C for 30 sec, and 72˚C for 30 sec. This process was cycled 40 times, followed by an extension at 72˚C for 10 min. The relative expression levels of circKMT2D, miR-210, Beclin1 and p62 were calculated using the 2-ΔΔCq method (23). U6 was used as the internal control for circKMT2D and miR-210, while GAPDH served as the internal control for Beclin1 and p62. The primer (Shanghai GeneChem) sequences used in the present study were as follows: circKMT2D forward, 5'-GATTTAATATTAACTGACG-3', reverse, 5'-GTTATGGATCCCGGCATGGC-3'; miR-210 forward, 5'-ATGCCTGTGCGTGTGA-3', reverse, 5'-GTGCGTGTCGTGGAGTC-3'; U6 forward, 5'-CGCTTCGGCAGCACATATACTA-3', reverse, 5'-CGCTTCACGAATTTGCGTGTCA-3'; Beclin1 forward, 5'-GATGGAAGGGTCTAAGACGTCCAA-3', reverse, 5'-TTTCGCCTGGGCTGTGGTAAG-3'; p62 forward, 5'-CCAGCACCAAGAGCACGGACAGCG-3', reverse, 5'-TGGGGAGAAGAAGGGGACCACGAA-3'; and GAPDH forward, 5'-AAGGTCATCCCTGAGCTGAAC-3' and reverse, 5'-ACGCCTGCTTCACCACCTTCT-3'.

Bioinformatic prediction and dual luciferase reporter assay. StarBase 2.0 (http://starbase.sysu.edu.cn) was used to predict whether the miRNAs could bind to circKMT2D. MG63 cells ($1.5x10^4$ cells/well) in the NC group, miR-210 mimic group and miR-210 inhibitor group were seeded into 6-well plates at logarithmic growth phase. Following 24 h culture, pmirGLO-circKMT2D-Mutant-type (Promega Corporation) and pmirGLO-circKMT2D-Wild-type (Promega Corporation) luciferase reporter vectors were used to transfect these cells. Transfection was performed using Lipofectamine 2000 (Invitrogen; Thermo Fisher Scientific, Inc.). Three replicate wells were set in each group. Following 24 h of incubation at 37˚C and 5% CO_2. The relative firefly and *Renilla* luciferase activities were detected using a Dual-Luciferase Reporter assay system (Promega Corporation). Firefly luciferase activity was normalized to that of *Renilla* luciferase.

Western blotting. Cells were harvested and lysed using RIPA buffer (Thermo Fisher Scientific, Inc.). Protein concentration was detected using a BCA kit (Beyotime Institute of Biotechnology). Proteins (20 μg) were separated by 10% SDS-PAGE and transferred to PVDF membranes. Membranes were washed three times with TBST (0.1%) and blocked with 5% non-fat milk for 2 h at room temperature. Membranes were incubated with rabbit anti-mouse Beclin1 (1:1,000; Cell Signaling Technology, Inc.) and p62 (1:1,000; Cell Signaling Technology, Inc.) primary antibodies for 12 h at 4˚C. Membranes were washed with TBST and were incubated with goat anti-rabbit secondary antibody (1:2,000, Beijing Solarbio) for 2 h at room temperature. Enhanced chemiluminescence chromogenic solution (Beijing Solarbio Science & Technology Co., Ltd.) was used to detect the signal on the membrane. The data were analyzed via densitometry and normalized to expression of the internal control GAPDH. Protein expression was evaluated using Image-Pro® Plus software (version 6.0; Media Cybernetics, Inc.).

Statistical analysis. The data were expressed as the means ± standard deviation. SPSS 19.0 software (IBM Corp.) was used for statistical analysis. Comparison between two groups was carried out using Student's t-test. Comparison between three groups was performed using ANOVA followed by Tukey's test. $P<0.05$ was considered to indicate a statistically significant difference.

Results

H_2O_2 treatment inhibits OS progression and decreases circKMT2D expression in OS cells. MG63 and U2OS cells were treated with H_2O_2, and cell viability, invasive ability and apoptosis were detected. The results demonstrated that MG63 and U2OS cells treated with H_2O_2 exhibited a significantly lower cell viability and invasive ability, and a significantly increased apoptotic rate compared with untreated cells (Fig. 1A-C). In addition, circKMT2D expression level was significantly decreased in H_2O_2-treated MG63 and U2OS cells compared with control cells (Fig. 1D).

circKMT2D knockdown accentuates H_2O_2-treated OS cell viability and invasion inhibition. Compared with the shNC group, MG63 and U2OS cells in the shcircKMT2D group exhibited a significantly lower circKMT2D expression level (Fig. 2A), indicating that circKMT2D was successfully knocked down in MG63 and U2OS cells. The results of CCK-8 assay, Transwell assay and apoptosis detection indicated that MG63 and U2OS cells in the shcircKMT2D group exhibited a significantly lower cell viability and invasion ability, and a significantly higher apoptotic rate compared with cells in the shNC group (Fig. 2B-D).

circKMT2D possesses binding sites for miR-210 and directly inhibits miR-210 expression. The binding site between circKMT2D and miR-210 was predicted by Starbase V2.0 and is illustrated in Fig. 3A. The results from dual luciferase reporter assay reported that, compared with the luciferase activity of wild-type circKMT2D in MG63 cells of the NC group, a significantly decreased luciferase activity was observed in the miR-210 mimic group, and a significantly increased luciferase activity was demonstrated in the miR-210 inhibitor group. However, compared with the luciferase activity of mutant circKMT2D in the NC group, no changes were observed in the

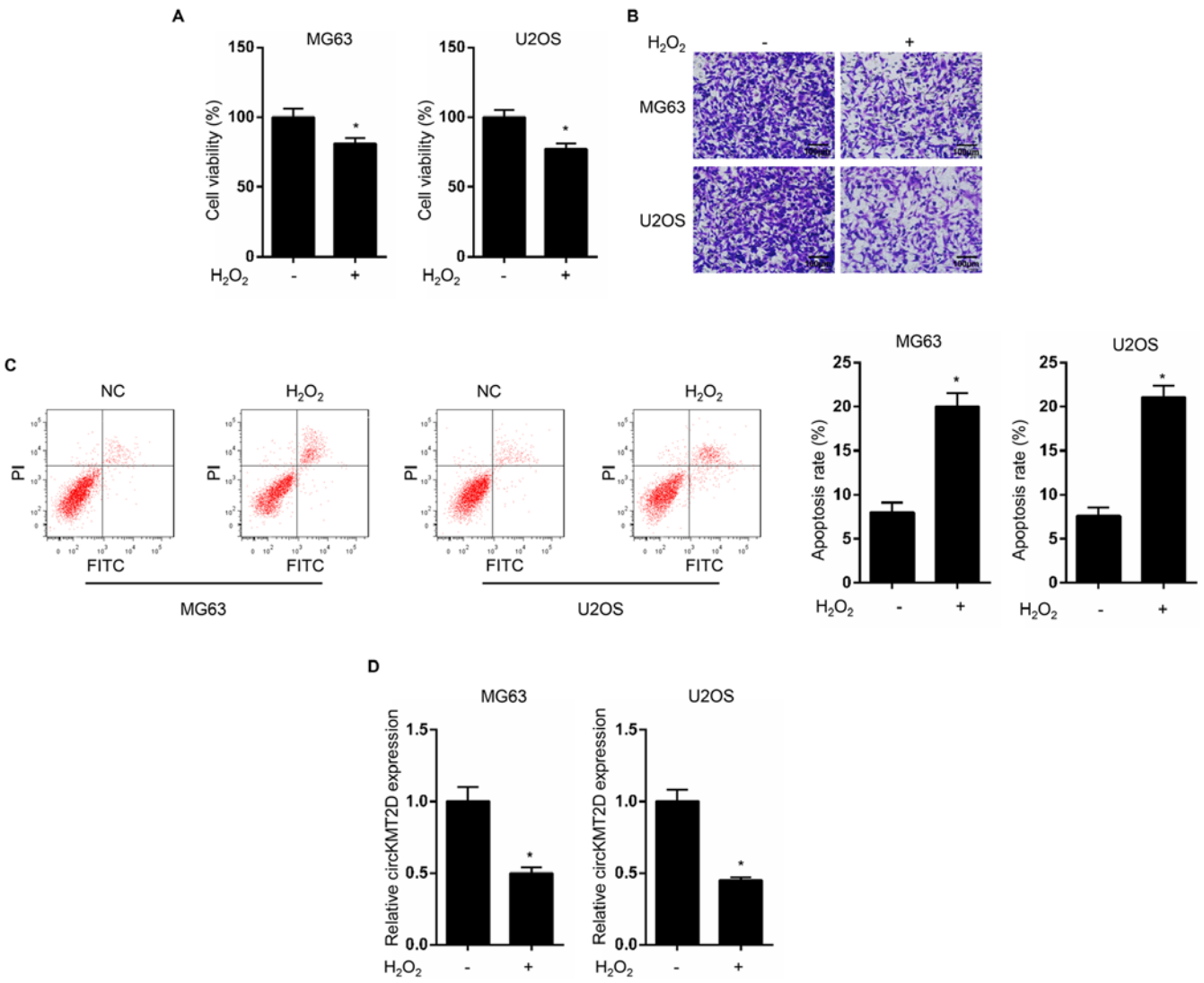

Figure 1. H_2O_2 treatment inhibited OS progression and decreased circKMT2D expression in OS cells. (A) MG63 and U2OS cells were treated with 100 μM H_2O_2 and cell viability was detected using Cell Counting Kit-8 assay. (B) After treatment with 100 μM H_2O_2, MG63 and U2OS cells invasive ability was measured by Transwell experiment. (Magnification, x100; scale bar, 100 μm). (C) MG63 and U2OS cell apoptosis rate was detected by flow cytometry following treatment with 100 μM H_2O_2 (D) circKMT2D expression in MG63 and U2OS cells was detected by reverse transcription quantitative PCR following treatment with 100 μM H_2O_2. $^*P<0.05$. NC, negative control; FITC, fluorescein isothiocyanate; PI, propidium iodide; H_2O_2, hydrogen peroxide.

miR-210 mimic and miR-210 inhibitor groups (Fig. 3B). Thus, miR-210 is a target gene of circKMT2D, and its expression is directly inhibited by circKMT2D.

To further verify the regulatory association between the two genes, MG63 cells were transfected with NC, miR-210 mimic and miR-210 inhibitor and the expression of circKMT2D and miR-210 was detected. The results demonstrated that, compared with the NC group, a significantly higher miR-210 expression and a significantly lower circKMT2D expression were found in the miR-210 mimic group. However, when compared with the NC group, MG63 cells transfected with miR-210 inhibitor exhibited a significantly lower miR-210 expression and a higher circKMT2D expression (Fig. 3C). In addition, MG63 cells in the pcDNA3.1-circKMT2D group exhibited a significantly higher circKMT2D expression and a significantly lower miR-210 expression compared with those in the shNC group; however, cells in the shcircKMT2D group exhibited a lower circKMT2D expression and a significantly increased miR-210 expression compared with those in the shNC group (Fig. 3D). These findings further confirmed that miR-210 expression may directly be inhibited by circKMT2D.

miR-210 silencing partially reverses the OS cell phenotype induced by circKMT2D knockdown. miR-210 expression in shNC, shcircKMT2D and shcircKMT2D + miR-210 inhibitor groups was assessed. A significanlty higher miR-210 expression was observed in the shcircKMT2D group compared with the shNC group. However, compared with the shcircKMT2D group, the expression of miR-210 was significantly decreased in the shcircKMT2D + miR-210 inhibitor group (Fig. 4A). Furthermore, compared with the shNC group, MG63 cells in the shcircKMT2D group exhibited a significantly lower cell viability and invasive ability, and a significantly higher apoptotic rate. However, MG63 cells in the shcircKMT2D + miR-210 inhibitor group exhibited a significantly higher cell viability and invasive ability, and a significantly lower

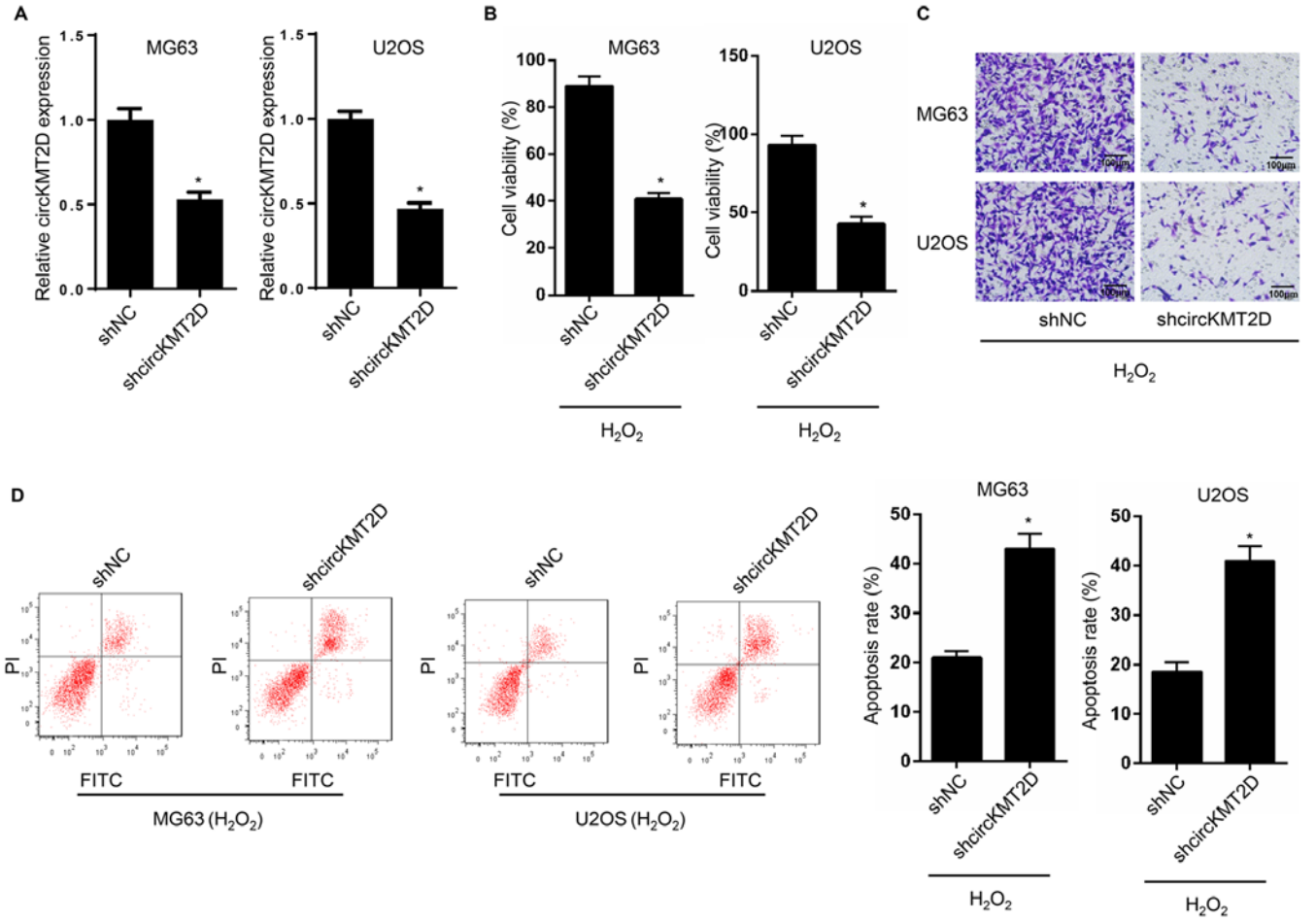

Figure 2. Knockdown of circKMT2D contributed to H_2O_2-induced OS cells viability and invasion inhibition. (A) MG63 and U2OS cells were transfected and circKMT2D expression was detected by reverse transcription quantitative PCR. (B) After transfection, MG63 and U2OS cell viability was evaluated using the Cell Counting Kit-8 assay. (C) After transfection, MG63 and U2OS cell invasion ability was detected by Transwell experiment (Magnification, x100; scale bar, 100 μm). (D) Following transfection, MG63 and U2OS cell apoptosis was detected by flow cytometry. *P<0.05. NC, negative control; FITC, fluorescein isothiocyanate; PI, propidium iodide; H_2O_2, hydrogen peroxide; sh, short hairpin.

apoptotic rate compared with those in the shcircKMT2D group (Fig. 4C and D).

miR-210 promotes OS cell autophagy. Beclin1 and p62 are genes associated with autophagy. In the present study, the expression of Beclin1 and p62 in MG63 cells was determined. The results from RT-qPCR demonstrated that MG63 cells in the miR-210 mimic group exhibited a significantly higher Beclin1 expression level and a significantly decreased p62 expression level compared with those in the NC group. However, compared with the NC group, a significantly lower Beclin1 expression level and a significantly decreased p62 expression level were observed in the miR-210 inhibitor group (Fig. 5A). These results were similar to those observed following western blotting analysis (Fig. 5B).

Autophagy inhibitor reverses the OS cell phenotype induced by miR-210 overexpression. The autophagy inhibitor 3-MA was used to treat MG63 cells transfected with miR-210 mimic. MG63 cells in the miR-210 mimic group exhibited a significantly decreased cell viability and invasive ability, and a significantly higher apoptotic rate compared with those in the NC group. However, compared with the miR-210 mimic group, a significantly elevated viability and invasive ability, and a significantly decreased apoptotic rate were observed in the miR-210 mimic + 3-MA group (Fig. 6A-C). These findings suggested that circKMT2D knockdown may contribute to H_2O_2-attenuated OS progression inhibition via the miR-210/autophagy pathway (Fig. 6D).

Discussion

OS is the most common primary malignant bone tumor. It mostly occurs in individuals under 20 years of age and is characterized by a rapid speed of deterioration (24,25). The prognosis of patients with OS is poor due to invasion and metastasis occurring in the early stages of the disease (26). Currently, OS treatment with chemotherapy has limited therapeutic efficacy as well as unsatisfactory side effects, in particular for relapsed and advanced OS (27). H_2O_2 is one main contributor of oxidative damage (28). Enhanced metabolic activity is one of the key features of tumor cells, and overproduction of H_2O_2 induces increased oxidative stress (29). Continuously elevated H_2O_2 levels can promote the survival of tumor cells and may therefore promote tumor cell ability to adapt to the tumor microenvironment. However, high levels of H_2O_2 can also

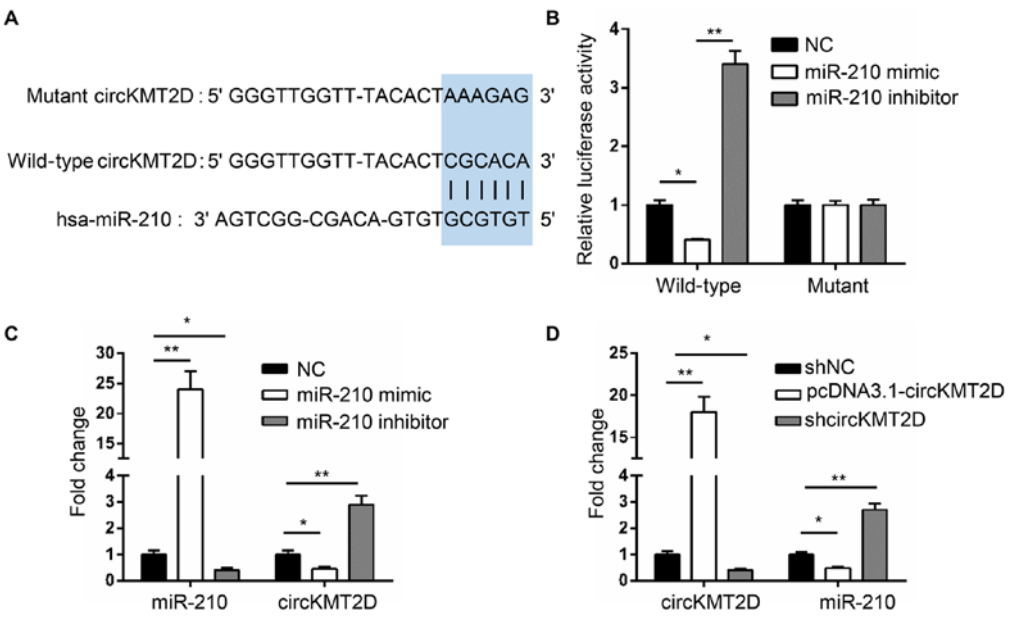

Figure 3. Expression of miR-210 and circKMT2D was mutually inhibited. (A) Binding site between circKMT2D and miR-210 was predicted by Starbase V2.0. (B) Dual luciferase reporter gene assay was used to analyze the regulatory relationship between circKMT2D and miR-210. (C and D) After transfection, circKMT2D and miR-210 expression in MG63 cells was detected by reverse transcription quantitative PCR. *P<0.05 and **P<0.01. NC, negative control; FITC, fluorescein isothiocyanate; PI, propidium iodide; H_2O_2, hydrogen peroxide; sh, short hairpin; miR, microRNA.

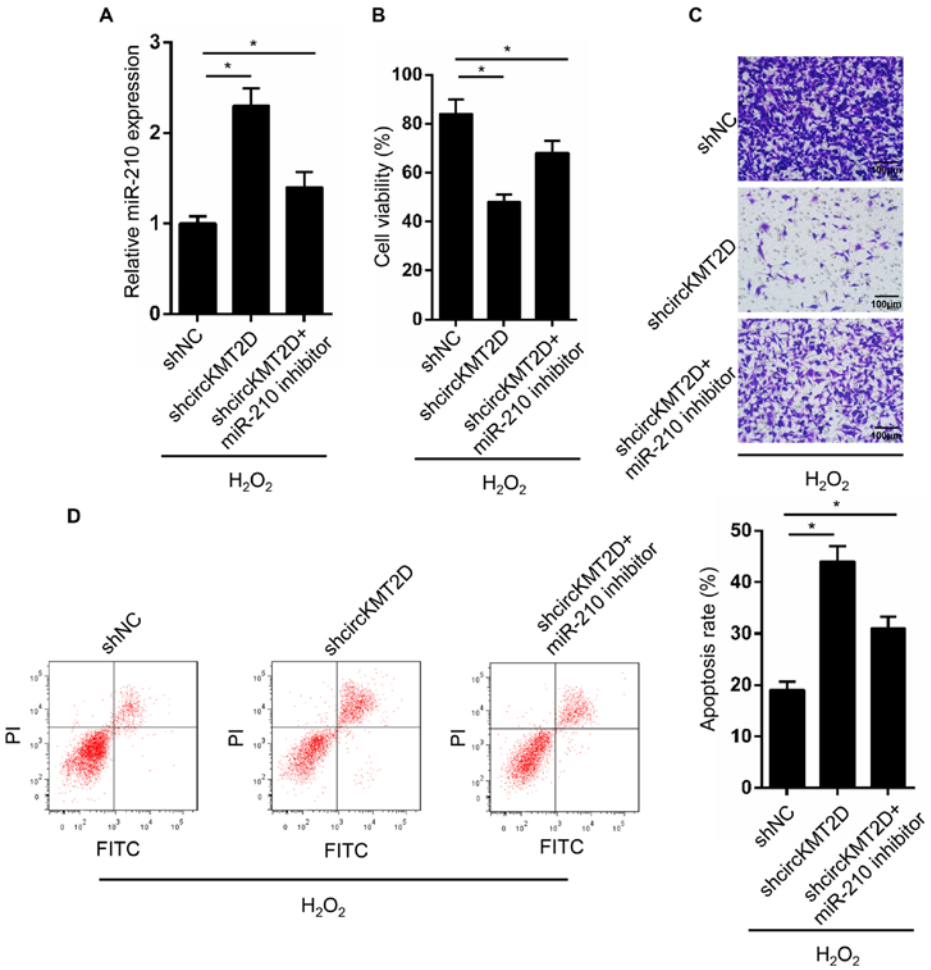

Figure 4. Silencing of miR-210 partially reversed OS cells phenotype induced by circKMT2D knockdown. (A) MG63 cells were transfected and miR-210 expression in MG63 cells of each group was detected by reverse transcription quantitative PCR. (B) After transfection, MG63 cell viability was evaluated using the Cell Counting Kit-8 assay. (C) After transfection, MG63 cell invasive ability was detected by Transwell experiment (Magnification, x100; scale bar, 100 μm). (D) After transfection, MG63 cell apoptosis was detected by flow cytometry. *P<0.05. NC, negative control; FITC, fluorescein isothiocyanate; PI, propidium iodide; H_2O_2, hydrogen peroxide; sh, short hairpin; miR, microRNA.

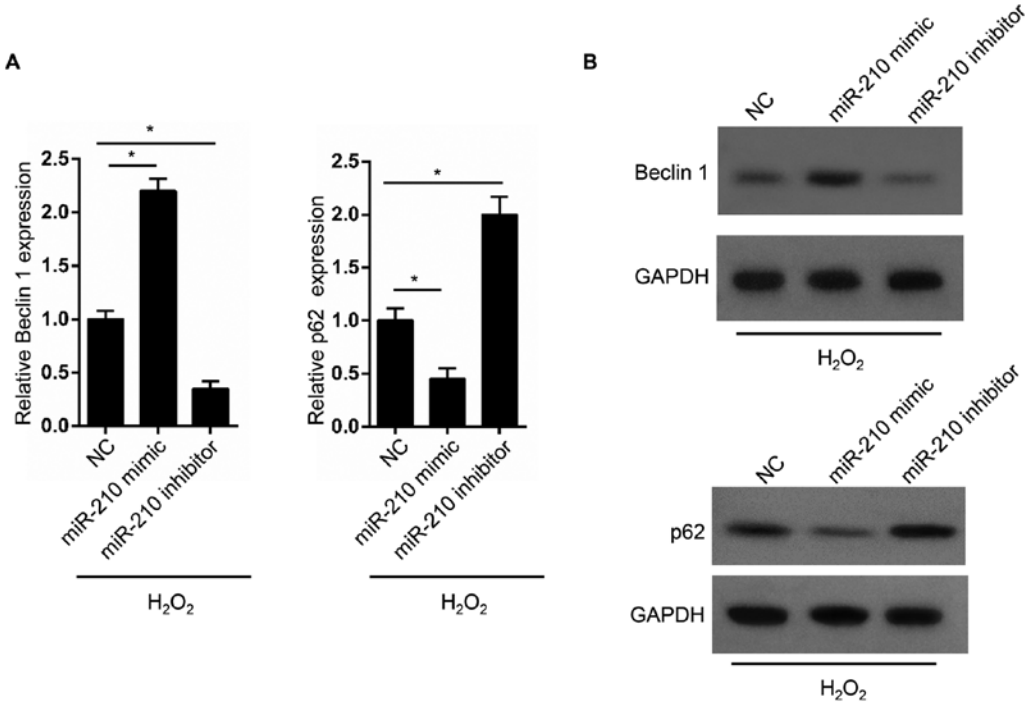

Figure 5. miR-210 promoted autophagy in OS cells. (A) MG63 cells were transfected and Beclin1 mRNA and p62 mRNA expression was detected by reverse transcription quantitative PCR. (B) After transfection, Beclin1 and p62 protein expression in was detected by western blotting. *P<0.05. NC, negative control; H_2O_2, hydrogen peroxide; miR, microRNA.

induce cell cycle arrest and cell death by apoptosis, thereby inhibiting the progression of tumors (30). Park (31) reported that 100 μM H_2O_2 suppressed the proliferation of lung cancer cells by arresting the cell cycle and inducing cells necrosis or apoptosis. In 2003, Ogawa *et al* (32) reported that potent oxidative stress caused by exogenous H_2O_2 induces the apoptosis of human OS cells. A recent study also demonstrated that treatment with H_2O_2 at a concentration of 100 μM resulted in a significant decrease in OS cell viability and an increase in apoptosis (9). The present study also confirmed that 100 μM H_2O_2 inhibited OS cell viability and invasive ability and promoted OS cell apoptosis. The underlying mechanism may involve the inhibition of circKMT2D expression.

To the best of our knowledge, the effects of circKMT2D on human tumors have not yet been reported. The present study demonstrated for the first time that circKMT2D may function as a cancer-promoting gene in OS. The regulatory effects of circRNAs on OS progression have been previously reported. Zhang *et al* (33) indicated that circUBAP2 enhanced the progression of OS by acting as a sponge of miR-143. Liu *et al* (34) reported that circNT5C2 promoted the metastasis of OS by targeting miR-448. However, circ0002052 can inhibit OS development by inhibiting OS cell proliferation and invasion, and by promoting apoptosis via targeting miR-1205 (15). In the present study, the cancer-promoting effects of circKMT2D in OS were discovered for the first time, and circKMT2D knockdown contributed to the inhibition of H_2O_2-attenuated OS progression by targeting miR-210.

Accumulating evidence indicates that miRNAs, as new types of diagnostic molecules and markers, have great prospects in targeted therapy of tumors, including OS (35,36). Fan *et al* (37) screened some key genes involved in the development of OS, including miRNAs, which may be related to the metastasis of OS. In several human malignancies, such as breast cancer, malignant peripheral nerve sheath tumors and renal cell carcinoma, miR-210 has been found to promote tumor development due to its upregulation and the enhancement of tumor cell proliferation or invasive ability (38-40). In OS, it has been reported that miR-210 functions as an oncogene. It promotes the migration and invasion of OS cells and is closely related to the aggressive development of OS (41,42). miR-210 has also been demonstrated to promote the dedifferentiation of OS cells (43). However, in the present study, rescue experiments revealed that the silencing of miR-210 partially reversed the H_2O_2-induced OS cell phenotypes induced by circKMT2D knockdown. miR-210 may therefore function as a tumor suppressor in OS and may serve as a potential target for targeted therapy and diagnosis of OS. Further experiments indicated that miR-210 may regulate the development of OS by interfering with autophagy in OS cells.

Autophagy is present in eukaryotes and plays an important role in cellular homeostasis, which is usually activated during adverse microenvironmental stress (44,45). During the autophagy process, organelles with damaged or aged structures and unwanted biomacromolecules are relocated to lysosomes for digestion and degradation, and autophagic products can be utilized by cell reconstruction to provide material basis and energy for cell survival (46,47). Numerous studies have demonstrated that the loss or inhibition of autophagy may lead to the development of a variety of tumors, including OS (48-50). A previous study has reported that the damage of lysosomal degradation function can lead to the accumulation of autophagosomes, whereas excess autophagosome accumulation and autophagy degradation blocking play important

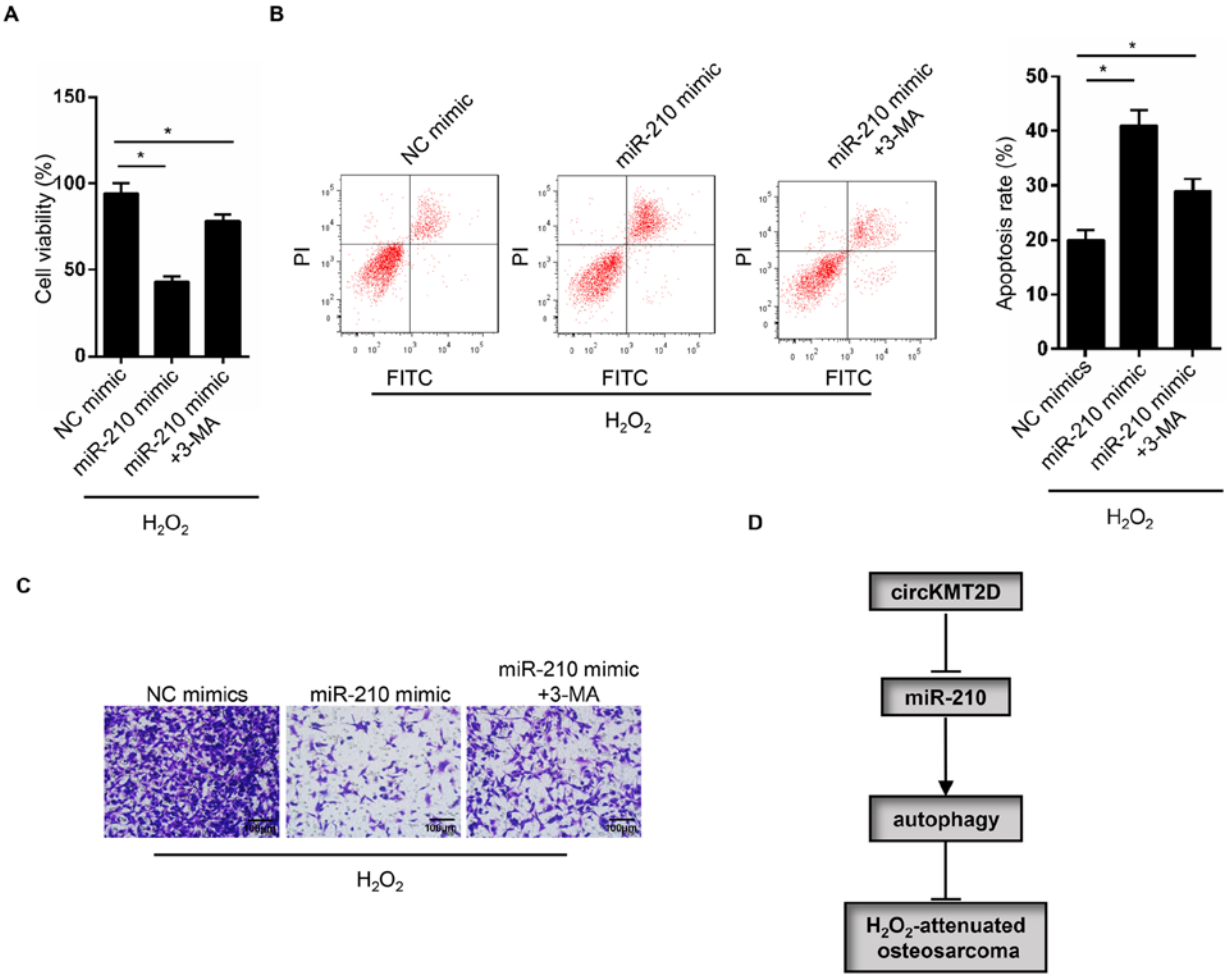

Figure 6. Autophagy inhibitor promoted the suppressed OS cell phenotype induced by miR-210 overexpression. (A) MG63 cells were transfected and treated with 3-MA. MG63 cell viability was evaluated using the Cell Counting Kit-8 assay. (B) MG63 cells were transfected and treated with 3-MA. MG63 cell apoptosis was detected by flow cytometry. (C) MG63 cells were transfected and treated with 3-MA. MG63 cell invasive ability was evaluated by Transwell experiment (Magnification, x100; scale bar, 100 μm). (D) Schematic diagram of findings from the present study. *P<0.05. NC, negative control; FITC, fluorescein isothiocyanate; PI, propidium iodide; H_2O_2, hydrogen peroxide; miR, microRNA; 3-MA, 3-methyladenine.

roles in OS cell death (51). Beclin-1 is a key regulatory protein in autophagy and its downregulation has been confirmed to promote the progression of several human cancers, including OS (52,53). Under normal conditions, the p62 level is very low in cells, since it is degraded in selective autophagy. However, p62 will accumulate in cells in the state of autophagy inhibition and autophagy defects (54). The accumulation of p62 can lead to the activation of NF-κB and stabilize Nrf2, whereas activated NF-κB can promote tumorigenesis and Nrf2 can enhance the tolerance of tumor cells to hypoxia-induced stress (55,56). In the present study, miR-210 overexpression elevated Beclin1 expression and decreased p62 expression in OS cells. miR-210 may therefore function by promoting autophagy to hinder the development of OS.

The PI3K/AKT/mTOR pathway has been demonstrated to be transitionally activated in OS, and the silencing of Wilms tumor gene 1 can inhibit the proliferation of OS cells by inactivating the PI3K/AKT pathway (57,58). Researchers have discovered that the enhancement of the PI3K/AKT/mTOR pathway inhibits doxorubicin-induced autophagy in OS cells and the diallyl disulfide-induced autophagic death of OS cells by inhibiting the PI3K/Akt/mTOR signaling pathway (59-61). It is therefore hypothesized that circKMT2D and miR-210 may affect autophagy through the PI3K/AKT/mTOR signaling pathway, thereby regulating the development of OS. This hypothesis will be further investigated.

In conclusion, the present study reported the potential molecular mechanisms of circKMT2D in H_2O_2-attenuated OS development. To the best of our knowledge, the present study was the first to demonstrate that circKMT2D knockdown contributed to the inhibition of H_2O_2-attenuated OS progression via the miR-210/autophagy pathway. These findings provided a theoretical basis for the treatment of OS with H_2O_2. In addition, circKMT2D may be considered as a novel target for the targeted therapy of OS, which will be further investigated in future studies.

Acknowledgements

Not applicable.

Funding

No funding was received.

Availability of data and materials

The datasets used and/or analyzed during the current study are available from the corresponding author on reasonable request.

Authors' contributions

JZ, ZL and XC designed the present study. MZ, CZ and DC performed the experiments. YH and JZ analysed the data and prepared the figures. JZ and XC drafted the initial manuscript. ZL reviewed and revised the manuscript. All authors read and approved the final manuscript.

Ethics approval and consent to participate

The present study was approved by Ethics Committee of The Third Affiliated Hospital of Soochow University.

Patient consent for publication

Not applicable.

Competing interests

The authors declare that they have no competing interests.

References

1. Yang L, Ge D, Chen X, Qiu J, Yin Z, Zheng S and Jiang C: FOXP4-AS1 participates in the development and progression of osteosarcoma by downregulating LATS1 via binding to LSD1 and EZH2. Biochem Biophys Res Commun 502: 493-500, 2018.
2. Lin YH, Jewell BE, Gingold J, Lu L, Zhao R, Wang LL and Lee DF: Osteosarcoma: Molecular Pathogenesis and iPSC Modeling. Trends Mol Med 23: 737-755, 2017.
3. Bashur L and Zhou G: Cancer stem cells in osteosarcoma. Case Orthop J 10: 38-42, 2013.
4. Wang Z, Li B, Ren Y and Ye Z: T-cell-based immunotherapy for osteosarcoma: Challenges and opportunities. Front Immunol 7: 353, 2016.
5. He C, Sun J, Liu C, Jiang Y and Hao Y: Elevated H3K27me3 levels sensitize osteosarcoma to cisplatin. Clin Epigenetics 11: 8, 2019.
6. Fridovich I: Oxygen free radicals and tissue damage: Chairman's introduction. Ciba Found Symp: 1-4, 1978.
7. Dong K, Yang C, Yan Y, Wang P, Sun Y, Wang K, Lu T, Chen Q, Zhang Y, Xing J and Dong Y: Investigation of the intracellular oxidative stress amplification, safety and anti-tumor effect of a kind of novel redox-responsive micelle. J Mater Chem B 6: 1105-1117, 2018.
8. Hahn HJ, Kim KB, An IS, Ahn KJ and Han HJ: Protective effects of rosmarinic acid against hydrogen peroxideinduced cellular senescence and the inflammatory response in normal human dermal fibroblasts. Mol Med Rep 16: 9763-9769, 2017.
9. Wang Y, Wang W and Qiu E: Protection of oxidative stress induced apoptosis in osteosarcoma cells by dihydromyricetin through down-regulation of caspase activation and up-regulation of BcL-2. Saudi J Biol Sci 24: 837-842, 2017.
10. Pei W, Tao L, Zhang LW, Zhang S, Cao J, Jiao Y, Tong J and Nie J: Circular RNA profiles in mouse lung tissue induced by radon. Environ Health Prev Med 22: 36, 2017.
11. Zhang HD, Jiang LH, Sun DW, Hou JC and Ji ZL: CircRNA: A novel type of biomarker for cancer. Breast Cancer 25: 1-7, 2018.
12. Barrett SP and Salzman J: Circular RNAs: Analysis, expression and potential functions. Development 143: 1838-1847, 2016.
13. Salmena L, Poliseno L, Tay Y, Kats L and Pandolfi PP: A ceRNA hypothesis: The Rosetta Stone of a hidden RNA language? Cell 146: 353-358, 2011.
14. Chen L, Zhang S, Wu J, Cui J, Zhong L, Zeng L and Ge S: circRNA_100290 plays a role in oral cancer by functioning as a sponge of the miR-29 family. Oncogene 36: 4551-4561, 2017.
15. Wu Z, Shi W and Jiang C: Overexpressing circular RNA hsa_circ_0002052 impairs osteosarcoma progression via inhibiting Wnt/β-catenin pathway by regulating miR-1205/APC2 axis. Biochem Biophys Res Commun 502: 465-471, 2018.
16. Huang L, Chen M, Pan J and Yu W: Circular RNA circNASP modulates the malignant behaviors in osteosarcoma via miR-1253/FOXF1 pathway. Biochem Biophys Res Commun 500: 511-517, 2018.
17. Li Z, Xuan W, Huang L, Chen N, Hou Z, Lu B, Wen C and Huang S: Claudin 10 acts as a novel biomarker for the prognosis of patients with ovarian cancer. Oncol Lett 20: 373-381, 2020.
18. Yang X, Shi L, Yi C, Yang Y, Chang L and Song D: MiR-210-3p inhibits the tumor growth and metastasis of bladder cancer via targeting fibroblast growth factor receptor-like 1. Am J Cancer Res 7: 1738-1753, 2017.
19. Liu S, Jiang T, Zhong Y and Yu Y: miR-210 inhibits cell migration and invasion by targeting the brain-derived neurotrophic factor in glioblastoma. J Cell Biochem: Feb 11, 2019 (Epub ahead of print).
20. Tan W, Lim SG and Tan TM: Up-regulation of microRNA-210 inhibits proliferation of hepatocellular carcinoma cells by targeting YES1. World J Gastroenterol 21: 13030-13041, 2015.
21. Gulino R, Forte S, Parenti R, Memeo L and Gulisano M: MicroRNA and pediatric tumors: Future perspectives. Acta Histochem 117: 339-354, 2015.
22. Zhao XH, Xu ZR, Zhang Q and Yang YM: Simvastatin protects human osteosarcoma cells from oxidative stress-induced apoptosis through mitochondrial-mediated signaling. Mol Med Rep 5: 483-488, 2012.
23. Livak KJ and Schmittgen TD: Analysis of relative gene expression data using real-time quantitative PCR and the 2(-Delta Delta C(T)) method. Methods 25: 402-408, 2001.
24. Zhang Y, Wang F, Li M, Yu Z, Qi R, Ding J, Zhang Z and Chen X: Self-stabilized hyaluronate nanogel for intracellular codelivery of doxorubicin and cisplatin to osteosarcoma. Adv Sci (Weinh) 5: 1700821, 2018.
25. Li S, Zhang T, Xu W, Ding J, Yin F, Xu J, Sun W, Wang H, Sun M, Cai Z and Hua Y: Sarcoma-targeting peptide-decorated polypeptide nanogel intracellularly delivers shikonin for upregulated osteosarcoma necroptosis and diminished pulmonary metastasis. Theranostics 8: 1361-1375, 2018.
26. Durfee RA, Mohammed M and Luu HH: Review of osteosarcoma and current management. Rheumatol Ther 3: 221-243, 2016.
27. Zhang Y, Cai L, Li D, Lao YH, Liu D, Li M, Ding J and Chen X: Tumor microenvironment-responsive hyaluronate-calcium carbonate hybrid nanoparticle enables effective chemotherapy for primary and advanced osteosarcomas. Nano Res 11: 4806-4822, 2018.
28. Wu PF, Long LH, Zeng JH, Guan XL, Zhou J, Jin Y, Ni L, Wang F, Chen JG and Xie N: Protection of L-methionine against H_2O_2-induced oxidative damage in mitochondria. Food Chem Toxicol 50: 2729-2735, 2012.
29. Glasauer A and Chandel NS: Targeting antioxidants for cancer therapy. Biochem Pharmacol 92: 90-101, 2014.
30. Lennicke C, Rahn J, Lichtenfels R, Wessjohann LA and Seliger B: Hydrogen peroxide-production, fate and role in redox signaling of tumor cells. Cell Commun Signal 13: 39, 2015.
31. Park WH: Hydrogen peroxide inhibits the growth of lung cancer cells via the induction of cell death and G1phase arrest. Oncol Rep 40: 1787-1794, 2018.
32. Ogawa Y, Takahashi T, Kobayashi T, Kariya S, Nishioka A, Mizobuchi H, Noguchi M, Hamasato S, Tani T, Seguchi H, *et al*: Mechanism of hydrogen peroxide-induced apoptosis of the human osteosarcoma cell line HS-Os-1. Int J Mol Med 12: 459-463, 2003.
33. Zhang H, Wang G, Ding C, Liu P, Wang R, Ding W, Tong D, Wu D, Li C, Wei Q, *et al*: Increased circular RNA UBAP2 acts as a sponge of miR-143 to promote osteosarcoma progression. Oncotarget 8: 61687-61697, 2017.
34. Liu X, Zhong Y, Li J and Shan A: Circular RNA circ-NT5C2 acts as an oncogene in osteosarcoma proliferation and metastasis through targeting miR-448. Oncotarget 8: 114829-114838, 2017.
35. Liu H, Li P, Chen L, Jian C, Li Z and Yu A: MicroRNAs as a novel class of diagnostic biomarkers for the detection of osteosarcoma: A meta-analysis. OncoTargets Ther 10: 5229-5236, 2017.
36. Fujiwara T, Uotani K, Yoshida A, Morita T, Nezu Y, Kobayashi E, Yoshida A, Uehara T, Omori T, Sugiu K, *et al*: Clinical significance of circulating miR-25-3p as a novel diagnostic and prognostic biomarker in osteosarcoma. Oncotarget 8: 33375-33392, 2017.

37. Fan H, Lu S, Wang S and Zhang S: Identification of critical genes associated with human osteosarcoma metastasis based on integrated gene expression profiling. Mol Med Rep 20: 915-930, 2019.
38. Zhang Y, Yan J, Wang L, Dai H, Li N, Hu W and Cai H: HIF-1α promotes breast cancer cell MCF-7 proliferation and invasion through regulating miR-210. Cancer Biother Radiopharm 32: 297-301, 2017.
39. Wang Z, Yin B, Wang B, Ma Z, Liu W and Lv G: MicroRNA-210 promotes proliferation and invasion of peripheral nerve sheath tumor cells targeting EFNA3. Oncol Res 21: 145-154, 2013.
40. Redova M, Poprach A, Besse A, Iliev R, Nekvindova J, Lakomy R, Radova L, Svoboda M, Dolezel J, Vyzula R and Slaby O: MiR-210 expression in tumor tissue and in vitro effects of its silencing in renal cell carcinoma. Tumour Biol 34: 481-491, 2013.
41. Cai H, Lin L, Cai H, Tang M and Wang Z: Prognostic evaluation of microRNA-210 expression in pediatric osteosarcoma. Med Oncol 30: 499, 2013.
42. Liu X, Zhang C, Wang C, Sun J, Wang D, Zhao Y and Xu X: miR-210 promotes human osteosarcoma cell migration and invasion by targeting FGFRL1. Oncol Lett 16: 2229-2236, 2018.
43. Zhang H, Mai Q and Chen J: MicroRNA-210 is increased and it is required for dedifferentiation of osteosarcoma cell line. Cell Biol Int 41: 267-275, 2017.
44. Ebner P, Poetsch I, Deszcz L, Hoffmann T, Zuber J and Ikeda F: The IAP family member BRUCE regulates autophagosome-lysosome fusion. Nat Commun 9: 599, 2018.
45. Ding WX, Ni HM, Gao W, Hou YF, Melan MA, Chen X, Stolz DB, Shao ZM and Yin XM: Differential effects of endoplasmic reticulum stress-induced autophagy on cell survival. J Biol Chem 282: 4702-4710, 2007.
46. Kim EH, Sohn S, Kwon HJ, Kim SU, Kim MJ, Lee SJ and Choi KS: Sodium selenite induces superoxide-mediated mitochondrial damage and subsequent autophagic cell death in malignant glioma cells. Cancer Res 67: 6314-6324, 2007.
47. Terman A, Gustafsson B and Brunk UT: Autophagy, organelles and ageing. J Pathol 211: 134-143, 2007.
48. Li L, Li Y, Zhao J, Fan S, Wang L and Li X: CX-5461 induces autophagy and inhibits tumor growth via mammalian target of rapamycin-related signaling pathways in osteosarcoma. Onco Targets Ther 9: 5985-5997, 2016.
49. Ranjan A and Srivastava SK: Penfluridol suppresses pancreatic tumor growth by autophagy-mediated apoptosis. Sci Rep 6: 26165, 2016.
50. Li C, Xu H, Chen X, Chen J, Li X, Qiao G, Tian Y, Yuan R, Su S, Liu X and Lin X: Aqueous extract of clove inhibits tumor growth by inducing autophagy through AMPK/ULK pathway. Phytother Res 33: 1794-1804, 2019.
51. Xu J, Wang H, Hu Y, Zhang YS, Wen L, Yin F, Wang Z, Zhang Y, Li S, Miao Y, *et al*: Inhibition of CaMKIIα activity enhances antitumor effect of fullerene C60 nanocrystals by suppression of autophagic degradation. Adv Sci (Weinh) 6: 1801233, 2019.
52. Zhou W, Yue C, Deng J, Hu R, Xu J, Feng L, Lan Q, Zhang W, Ji D, Wu J, *et al*: Autophagic protein Beclin 1 serves as an independent positive prognostic biomarker for non-small cell lung cancer. PLoS One 8: e80338, 2013.
53. Xu R, Liu S, Chen H and Lao L: MicroRNA-30a downregulation contributes to chemoresistance of osteosarcoma cells through activating Beclin-1-mediated autophagy. Oncol Rep 35: 1757-1763, 2016.
54. Mathew R, Karp CM, Beaudoin B, Vuong N, Chen G, Chen HY, Bray K, Reddy A, Bhanot G, Gelinas C, *et al*: Autophagy suppresses tumorigenesis through elimination of p62. Cell 137: 1062-1075, 2009.
55. Lan SH, Wu SY, Zuchini R, Lin XZ, Su IJ, Tsai TF, Lin YJ, Wu CT and Liu HS: Autophagy suppresses tumorigenesis of hepatitis B virus-associated hepatocellular carcinoma through degradation of microRNA-224. Hepatology 59: 505-517, 2014.
56. Cheong H, Wu J, Gonzales LK, Guttentag SH, Thompson CB and Lindsten T: Analysis of a lung defect in autophagy-deficient mouse strains. Autophagy 10: 45-56, 2014.
57. Graziano AC, Cardile V, Avola R, Vicario N, Parenti C, Salvatorelli L, Magro G and Parenti R: Wilms' tumor gene 1 silencing inhibits proliferation of human osteosarcoma MG-63 cell line by cell cycle arrest and apoptosis activation. Oncotarget 8: 13917-13931, 2017.
58. Zhang J, Yu XH, Yan YG, Wang C and Wang WJ: PI3K/Akt signaling in osteosarcoma. Clin Chim Acta 444: 182-192, 2015.
59. Perry JA, Kiezun A, Tonzi P, Van Allen EM, Carter SL, Baca SC, Cowley GS, Bhatt AS, Rheinbay E, Pedamallu CS, *et al*: Complementary genomic approaches highlight the PI3K/mTOR pathway as a common vulnerability in osteosarcoma. Proc Natl Acad Sci USA 111: E5564-E5573, 2014.
60. Wang L, Tang B, Han H, Mao D, Chen J, Zeng Y and Xiong M: miR-155 affects osteosarcoma MG-63 cell autophagy induced by adriamycin through regulating PTEN-PI3K/AKT/mTOR signaling pathway. Cancer Biother Radiopharm 33: 32-38, 2018.
61. Yue Z, Guan X, Chao R, Huang C, Li D, Yang P, Liu S, Hasegawa T, Guo J and Li M: Diallyl disulfide induces apoptosis and autophagy in human osteosarcoma MG-63 cells through the PI3K/Akt/mTOR pathway. Molecules 24: 2665, 2019.